Nanosized Carbon Black Combined with Ni$_2$O$_3$ as "Universal" Catalysts for Synergistically Catalyzing Carbonization of Polyolefin Wastes to Synthesize Carbon Nanotubes and Application for Supercapacitors

Xin Wen,[†] Xuecheng Chen,[†,‡] Nana Tian,[†] Jiang Gong,[†] Jie Liu,[†] Mark H. Rümmeli,[§,∥] Paul K. Chu,[⊥] Ewa Mijiwska,[‡] and Tao Tang*,[†]

[†]State Key Laboratory of Polymer Physics and Chemistry, Changchun Institute of Applied Chemistry, Changchun, Jilin 130022, China

[‡]Institute of Chemical and Environment Engineering, West Pomeranian University of Technology, Szczecin ul. Pulaskiego 10, 70-322 Szczecin, Poland

[§]IBS Center for Integrated Nanostructure Physics, Institute for Basic Science (IBS), Daejon 305-701, Republic of Korea

[∥]Department of Energy Science, Department of Physics, Sungkyunkwan University, Suwon 440-746, Republic of Korea

[⊥]Department of Physics and Materials Science, City University of Hong Kong, Tat Chee Avenue, Kowloon, Hong Kong, China

Ⓢ Supporting Information

ABSTRACT: The catalytic carbonization of polyolefin materials to synthesize carbon nanotubes (CNTs) is a promising strategy for the processing and recycling of plastic wastes, but this approach is generally limited due to the selectivity of catalysts and the difficulties in separating the polyolefin mixture. In this study, the influence of nanosized carbon black (CB) and Ni$_2$O$_3$ as a novel combined catalyst system on catalyzing carbonization of polypropylene (PP), polyethylene (PE), polystyrene (PS) and

their blends was investigated. We showed that this combination was efficient to promote the carbonization of these polymers to produce CNTs with high yields and of good quality. Catalytic pyrolysis and model carbonization experiments indicated that the carbonization mechanism was attributed to the synergistic effect of the combined catalysts rendered by CB and Ni$_2$O$_3$: CB catalyzed the degradation of PP, PE, and PS to selectively produce more aromatic compounds, which were subsequently dehydrogenated and reassembled into CNTs via the catalytic action of CB together with Ni particles. Moreover, the performance of the synthesized CNTs as the electrode of supercapacitor was investigated. The supercapacitor displayed a high specific capacitance as compared to supercapacitors using commercial CNTs and CB. This difference was attributed to the relatively larger specific surface areas of our synthetic CNTs and their more oxygen-containing groups.
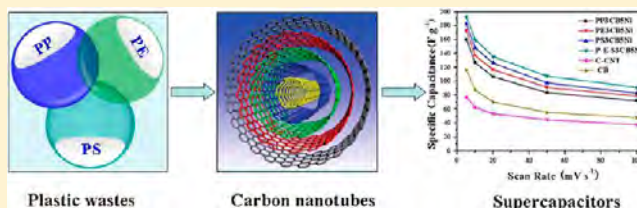
1. INTRODUCTION

On the back of growing environmental awareness, the processing and recycling of plastic wastes has attracted a lot of attention in recent years.[1−3] In particular, being one of the most popular plastics, polyolefin makes up a considerable portion of polymer wastes.[4] Currently landfills and incineration are the two common measures to dispose of plastic wastes. However, continuous cost increases, long-term environmental concerns, and diminishing space for landfills make alternative treatment options much needed.

Carbon nanotubes (CNTs), one of the most important nanostructured carbon materials, have attracted much interest since their discovery due to the variety in structure, unique properties, and potential applications.[5−9] For example, CNTs can be used as electrodes for supercapacitors due to their high mechanical resilience, interconnnected pore structure, high electrical conductivity, and environmental friendliness.[10−13] Thus, much effort has been made to synthesize CNTs by different

methods,[14−16] primarily using arc evaporation,[17] laser vaporization,[18,19] and chemical vapor deposition (CVD).[20,21] However, most of these techniques employ small molecules as carbon sources, which are energy-consuming and resource intensive.[22,23] Considering the rich carbon content in polyolefins, its use as a carbon feedstock could be a promising strategy for the large-scale production of CNTs. Generally the conversion of polyolefin into CNTs requires two steps. Polyolefin is first catalytically degraded into organic compounds with lower carbon numbers, then these small molecules are dehydrogenated to produce carbon products. During the above process, the key is to find appropriate catalysts for promoting the degradation of polyolefin as well as the carbonization of the byproducts. Some excellent work has been

Table 1. Carbon Yield of Polymer Composites Burned in a Crucible at 700 °C

	sample	polyolefins (wt%)		PS (wt%)	CB (wt%)	Ni$_2$O$_3$ (wt%)	yield of carbon[a] (wt%)
		PP	PE				
1−1	PP5Ni	100				5	5.8 ± 0.4
1−2	PP0.5CB5Ni	100			0.5	5	17.9 ± 0.7
1−3	PP1CB5Ni	100			1	5	25.5 ± 0.9
1−4	PP3CB5Ni	100			3	5	36.2 ± 1.2
1−5	PP5CB5Ni	100			5	5	42.1 ± 1.3
1−6	PP5CB	100			5		0.7 ± 0.2
2−1	PE5Ni		100			5	5.3 ± 0.2
2−2	PE1CB5Ni		100		1	5	19.6 ± 0.3
2−3	PE3CB5Ni		100		3	5	30.5 ± 0.6
2−4	PE5CB5Ni		100		5	5	36.4 ± 1.0
2−5	PE5CB		100		5		0.8 ± 0.3
3−1	PS5Ni			100		5	3.2 ± 0.2
3−2	PS1CBNi			100	1	5	11.8 ± 0.5
3−3	PS3CB5Ni			100	3	5	18.9 ± 0.6
3−4	PS5CB5Ni			100	5	5	25.6 ± 0.6
3−5	PS5CB			100	5		1.1 ± 0.3
4−1	PP-PS1CB5Ni	90		10	1	5	22.1 ± 0.5
4−2	PP-PS5CB5Ni	90		10	5	5	37.9 ± 0.7
4−3	PE-PS5CB5Ni		90	10	5	5	32.1 ± 1.1
4−4	P-E-S[b]1CB5Ni	26.9	56.3	16.8	1	5	16.1 ± 0.7
4−5	P-E-S3CB5Ni	26.9	56.3	16.8	3	5	26.3 ± 0.7
4−6	P-E-S5CB5Ni	26.9	56.3	16.8	5	5	31.6 ± 0.9

[a]Yield of carbon: the amounts of residual catalysts were subtracted. [b]P-E-S denotes as the mixture of PP, PE, and PS.

reported on the synthesis of CNTs from plastic wastes, but the main carbon source has focused on a single component of polyolefin, mainly from polypropylene (PP) or polyethylene (PE).[24−26] In our previous work,[27,28] a novel combined catalyst consisting of organically modified clay (OMC) and nickel catalysts (Ni-Cat), was found to effectively catalyze the carbonization of PP to synthesize CNTs. However, the catalytic behavior of polymers depends strongly on their chemical structure. As shown in Table S1 in the Supporting Information (SI), in spite of using the same catalysts composed of OMC and Ni-Cat, the yields of carbon from PP and PE systems can be as high as 47.3 and 34.1 wt %, respectively, but that from polystyrene (PS) is only 4.2 wt %. Furthermore, when some amount of PS is included in polyolefin blends, the CNTs yield becomes almost negligeable (less than 5 wt %). A similar trend was also observed for another type of combined catalyst comprising of H-form zeolite and Ni$_2$O$_3$[29] (SI Table S1). This may be ascribed to the influence of the composition of the degradation products with different chemical structure,[30,31] in which the carbonization reaction is difficult to achieve. It is well-known that PS is often included in polyolefin wastes, making it a difficult to separate each component from the mixture. Thus, the best solution for CNTs production from polyolefin wastes is to come up with a "universal" catalyst system, which not only promotes the efficient carbonization of PP, PE, and PS, but also ensures the carbonization of the degradation products from each component is not negatively influenced by the others.

Herein we demonstrate a novel type of "universal" combined catalyst consisting of nanosized carbon black (CB) and Ni$_2$O$_3$, which can efficiently catalyze the carbonization of PP, PE, and PS as well as their mixtures. Most importantly, the resultant carbon products are mainly composed of CNTs with a high yield. The efficient carbonization process is attributed to a synergistic catalysis between CB and Ni$_2$O$_3$, which plays an important role in controlling the degradation of these polymers

and subsequent carbonization of the degradation products into CNTs.

2. MATERIALS AND METHODS

2.1. Materials. Polypropylene powder (isotactic, T30s, $M_w = 2.89 \times 10^5$ g mol^{-1}, polydispersity = 3.45), polyethylene pellet (HDPE, 5000S, $M_w = 3.75 \times 10^5$ g mol^{-1}, polydispersity = 4.36) and polystyrene pellet (666D, $M_w = 2.72 \times 10^5$ g mol^{-1}, polydispersity = 3.28) were supplied by Daqing Petrochemical Co. Ltd. Nanosized carbon black was purchased from Linzi Qishun Chemical Co., with the original particle diameter of 17 nm. Ni$_2$O$_3$ was from Lingfeng Chemical Company with the average diameter of 250−300 nm. A type of commerical CNTs (C−CNT) was from Shenzhen Nanotech Port Co., Ltd. with the diameter of 40−60 nm and the length of 5−15 um.

2.2. Preparation of Polymer Composites. Polymer composites with different amounts of catalysts were prepared via melt compounding in a Haake mixer (Haake Rheomix 600, Karlsruhe, Germany) with a rotor speed of 60 rpm for 6 min. The compounding temperature was at 180 °C for PP, 160 °C for PE, 190 °C for PS, and 190 °C for their mixtures.

2.3. The Carbon Yield of Polymer Samples. A piece of sample about 6.0 ± 0.3 g was placed in a 30 mL crucible and burned with the flame of a gas lamp (Figure S1, SI). The yield of carbon was calculated by the mass of transformed carbon products divided by the polymer mass.

2.4. Catalytic Pyrolysis for Polymer Composites. About 5.0 ± 0.1 g samples were placed in a quartz tube and pyrolyzed at 700 °C. Gas chromatography (GC, SHIMADZU GC-14C) and gas chromatography−mass spectrometry (GC−MS, AGILENT 5975MSD) were used to measure the composition of gas and liquid products, respectively.

2.5. Model Experiments for Catalyzing Carbonization. 2.0 g Ni$_2$O$_3$ (or the mixture of Ni$_2$O$_3$ and CB, 50/50 by mass) was placed in the quartz tube at 700 °C. Ten mL of benzene,
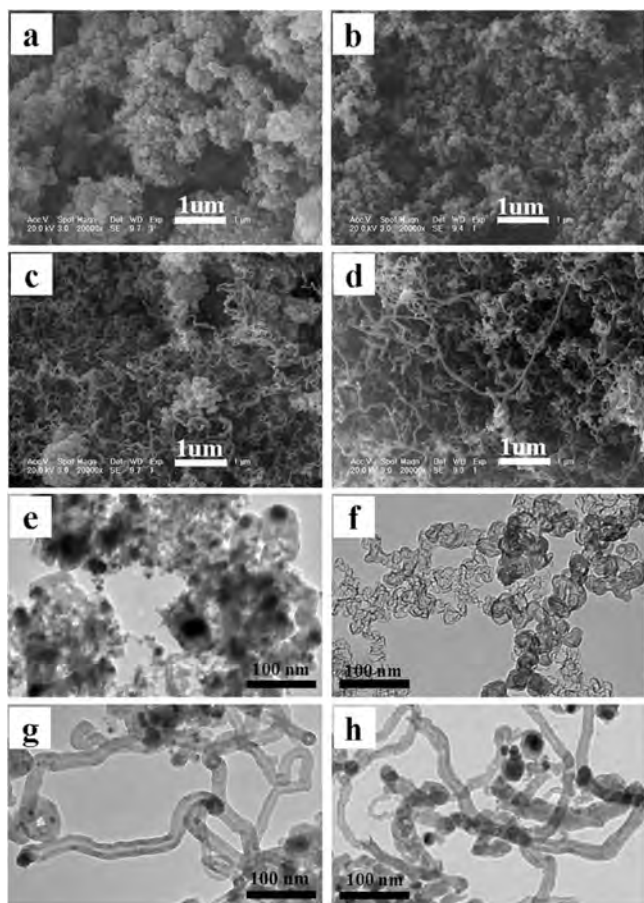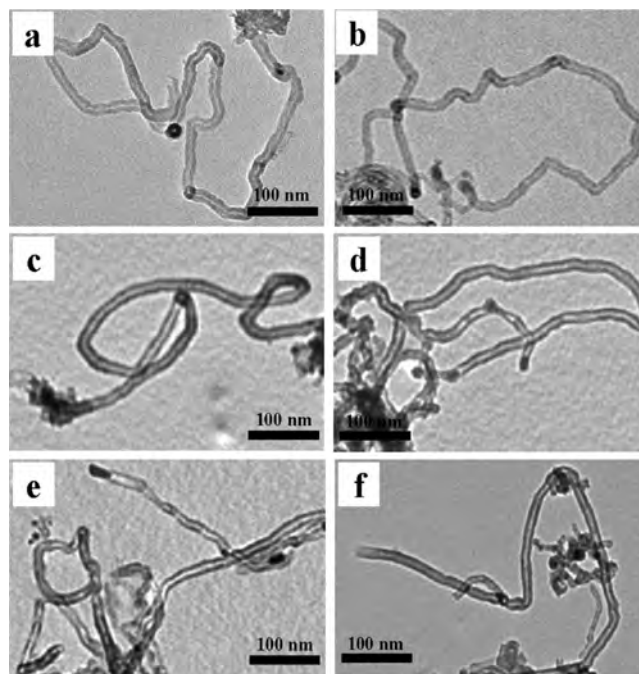
Figure 1. SEM and TEM images for the carbon products from PP/CB/Ni$_2$O$_3$ composites: (a, e) PP5Ni; (b, f) PP5CB; (c, g) PP1CB5Ni; and (d, h) PP5CB5Ni.

Figure 2. TEM images for the carbon products from PE/CB/Ni$_2$O$_3$ composites, PS/CB/Ni$_2$O$_3$ and P-E-S/CB/Ni$_2$O$_3$ composites: (a) PE1CB5Ni; (b) PE3CB5Ni; (c) PS1CB5Ni; (d) PS3CB5Ni; (e) P-E-S1CB5Ni; (f) P-E-S3CB5Ni.

toluene, ethylbenzene or xylene were, respectively, injected drop by drop into the quartz tube, and their steam promoted by the bubbling of N$_2$/H$_2$ mixture (90/10 by volume) with the rate of 50 mL/min. Then the residues were weighted by an analytical balance. Naphthalene was dissolved in benzene (3g/10 mL), then dropped under the same condition as the above liquids. The mass of carbon from benzene was subtracted according to the efficiency of benzene alone.

2.6. Characterization of Carbon Materials. The char morphologies were examined by field-emission scanning electron microscopy (FE-SEM, XL303SEM) and transmission electron microscope (TEM, JEM-1011) at 100 kV. The microstructure was investigated by X-ray diffraction (XRD) using a Bruker D8 diffractometer, operating at 40 kV and 200 mA with Cu Kα radiation (λ = 0.154 nm). The vibrational properties were characterized by a Renishaw 2000 model confocal microscopy Raman spectrometer using the 514.5 nm diode laser. Thermal gravimetric analysis (TGA) was performed using TA Instruments SDT Q600 in air at 10 °C/min.

To remove the residual Ni catalysts, the chars were purified using nitric acid at 140 °C for 4 h, then washed with deionized water and separated by centrifugation at 10 000 r/min and dried at 80 °C for 8 h in a vacuum oven.

The N$_2$ adsorption/desorption isotherms for carbon materials were acquired at liquid nitrogen temperature (77 K) on a Micromeritics ASAP 2010 M instrument, and the specific surface area and the average diameter of pores were calculated by BET metod and BJH method, respectively.

The surface element composition of carbon materials was characterized by means of X-ray photoelectron spectroscopy (XPS) carried out on a VGESCALAB MKII spectrometer using an Al Kα exciting radiation from an X-ray source operated at 10.0 kV and 10 mA.

2.7. Electrochemical Properties. The carbon materials, acetylene black, and poly(tetrafluoroethylene) were mixed in a mass ratio of 80:15:5 and dispersed in ethanol to produce a homogeneous paste. Then the mixture was pressed onto a piece of foamed Ni grid and dried at 80 °C for 8 h in a vacuum oven. All electrochemical measurements were performed under a three-electrode cell at room temperature: the Ni foam was used as the working electrode, and a Pt foil (1 cm^2) and a saturated calomel electrode (SCE) were as the counter and reference electrode, respectively; 6 M KOH aqueous solution was as the electrolyte. Cyclic voltammetry (CV) test was carried out by a CHI-605B type electrochemical workstation.

3. RESULTS AND DISCUSSION

3.1. Synergistic Effect of CB/Ni$_2$O$_3$ on Catalyzing PP, PE, and PS into CNTs. The effect of CB and Ni$_2$O$_3$ as combined catalysts on the carbonization of PP was initially investigated (samples from 1−1 to 1−6 in Table 1). The binary composites containing Ni$_2$O$_3$ or CB alone exhibited poor catalytic efficiency. Interestingly, the combination of CB and Ni$_2$O$_3$ promoted the carbonization of PP efficiently. The yield of carbon products increased dramatically with the CB content, and PP5CB5Ni exhibited the highest char yield (42.1 wt %).

The morphology of carbon products was examined by SEM and TEM (Figure 1). The residues from PP5Ni and PP5CB consisted mainly of amorphous block-like carbon (Figure 1a and b), but a large amount of long fiber-like nanostructures with diameters between 50 and 70 nm were observed from PP1CB5Ni and PP3CB5Ni (Figure 1c and d). TEM further
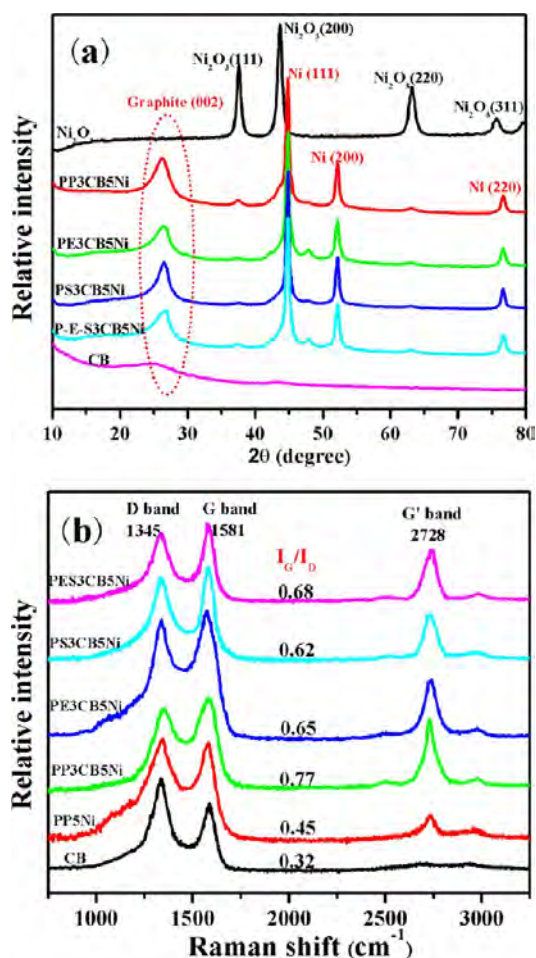
Figure 3. (a) XRD and (b) Raman spectra of carbon black and synthesized CNTs from polymer composites.

Figure 4. (a) Scheme of model experiment for catalytic carbonization using aromatic compounds as carbon sources; (b) Effect of catalysts on the yield of solid carbon products using aromatic compounds as carbon sources at 700 °C.

Figure 5. Schematic representation of the synergistic effect of combined catalysts on the carbonization of PP, PE and PS to form CNTs.

confirmed the different carbon microstructure, which consist of amorphous carbon enwrapped on nickel particles surfaces in PP5Ni (Figure 1e) and the added CB particles for PP5CB (Figure 1f), but the chars from PP1CB5Ni and PP3CB5Ni were a hollow tubular nanostructure (Figure 1g and h). These results suggest that the combined catalysts synergistically catalyze the carbonization of PP into CNTs.

Further investigations showed that the combined catalysts were also efficient to synthesize CNTs from PE, PS, and even polyolefin/PS blends. The yield trend of carbon in PE/CB/Ni_2O_3 was similar to that of PP/CB/Ni_2O_3, although the value was smaller to some extent (samples 2−1 to 2−5 in Table 1). Moreover, the combination also showed good catalytic efficiency in PS system (samples 3−1 to 3−5 in Table 1), and the highest yield reached to 25.6 wt % for PS5CB5Ni. More importantly, the combined catalysts could show a high yield of carbon in PP/PS, PE/PS, and PP/PE/PS blends (samples 4−1 to 4−6 in Table 1). When 10 wt % PS was added to PP5CB5Ni or PE5CB5Ni, the corresponding yield was still as high as 37.9 and 32.1 wt %, respectively. This result highlights that the inclusion of PS does not negatively affect the carbonization of PP and PE in the blends. In P-E-S systems (the weight percentage of PP/PE/PS was 26.9/56.3/16.8 according to their real-world proportion in polyolefin wastes[1]), the yield of carbon also increased with the CB content, and the highest value reached to 31.6 wt %, further indicating that the carbonization process of each constituent is independent in the
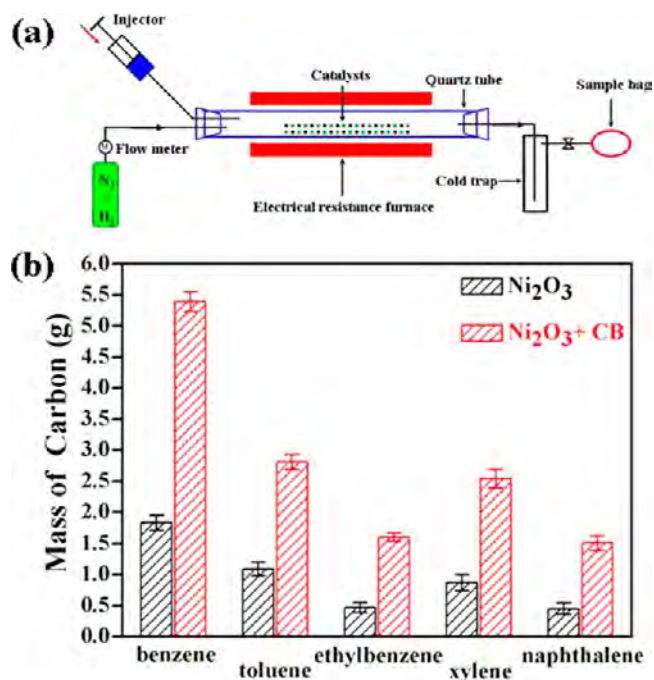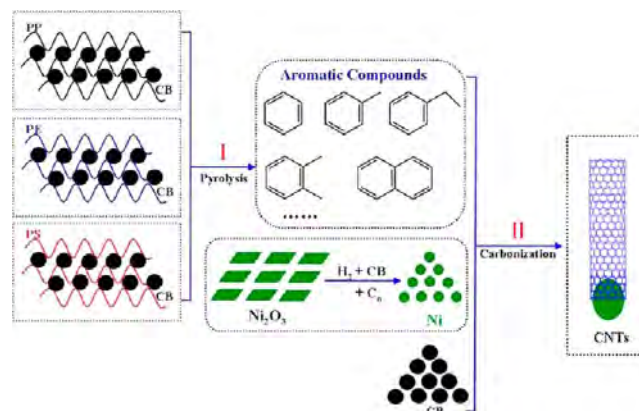
blends. The morphology of carbon products also exhibited long fiber-like nanostructures (SEM results in Figure S2a-2f, SI). The TEM images further confirmed that they were multiwalled CNTs, despite different diameter and wall thickness, which depend on the composition of polymers (Figure 2a−f). The results provide unequivocal evidence on the synergistic effect of CB and Ni_2O_3 on catalyzing carbonization of PE, PS, and polyolefin/PS blends into CNTs.

3.2. Analysis for the Quality of Synthesized CNTs. The quality of the as-produced CNTs was investigated by XRD, Raman spectroscopy and TGA, respectively. XRD showed that no signatures for Ni_2O_3 could be observed in all samples (Figure 3a). Instead three new peaks at 2θ = 44.7°, 52.0° and 76.5° were present, which can be assigned to pure Ni (111, 200, and 220 indices) and indicates the reduction of Ni_2O_3 during combustion.[32−34] In addition, the graphite peaks at 25.7° were
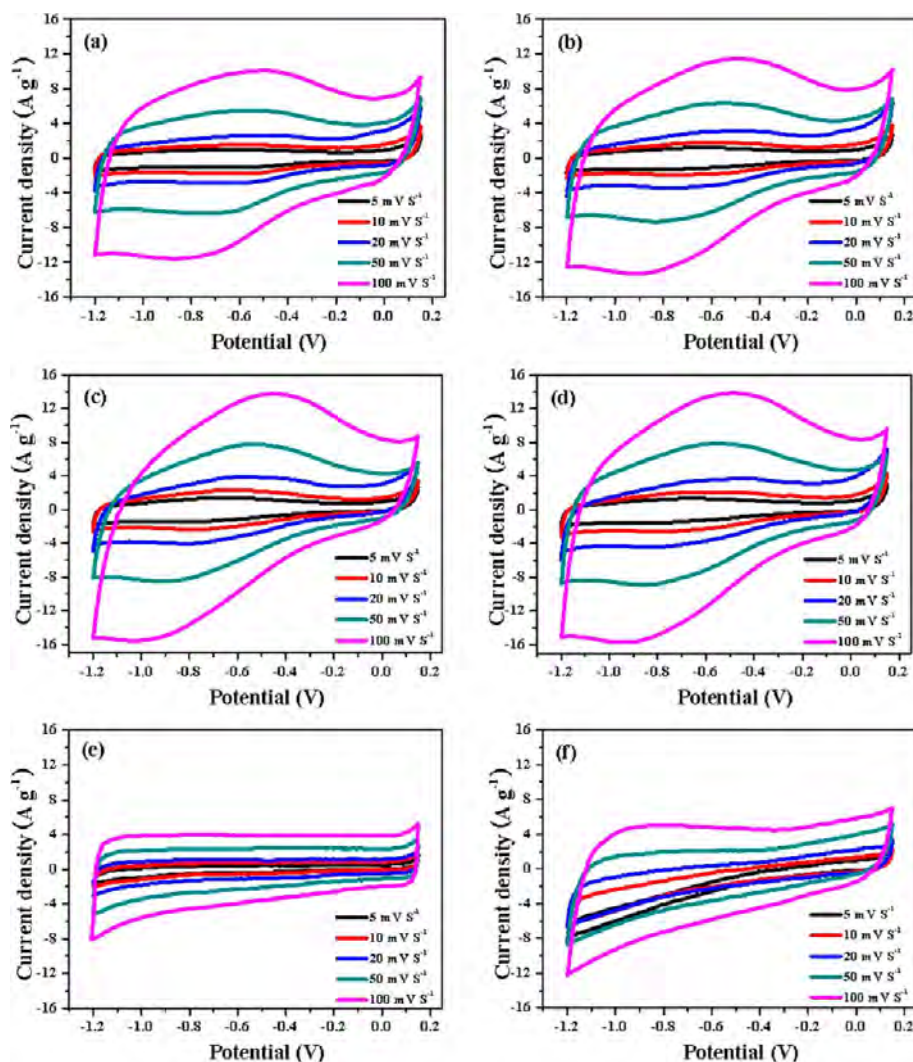
Figure 6. CV curves at different scan rates of the CNTs from (a) PP3CB5Ni, (b) PE3CB5Ni, (c) PS3CB5Ni, (d) P-E-S3CB5Ni; (e) C−CNTs; and (f) CB.

much stronger as compared to the reference CB signal, indicating the carbonization process forms enhanced graphitic carbon[35] in agreement with the TEM studies showing CNTs.

Raman results further confirmed graphitization during the carbonization process (Figure 3b). Since the D band (1345 cm^{-1}) and G band (1581 cm^{-1}) provide information on the disorder and crystallinity of sp^2 carbon materials, respectively, their intensity ratio (I_G/I_D) is often used to quantify how crystalline sp^2-hybridized carbon systems are.[36] The I_G/I_D ratios from carbon black and PP5Ni were rather low, concomitant with much of the sample containing amorphous carbon. The I_G/I_D ratio for the as produced carbons was noticeably higher, indicating higher crystallization (viz. CNT formation). Moreover, the G′ (2728 cm^{-1}) band is indicative of long-range order and arises from a two-phonon, second order scattering process, which represents a more accurate measurement of CNT quality or purity.[37,38] It is apparent that the $I_{G'}$ (the intensity of G′) of the synthesized carbons was much stronger than that from carbon black and PP5Ni.

TGA was also used to evaluate the graphitic nature and purity of the synthesized CNTs. Their TGA curves shifted significantly to a higher temperature range than that for CB, indicating the higher thermal stability (Figure S3a, SI). Furthermore, the derivative

thermogram (DTG) curves of synthesized CNTs exhibted a sharp peak, and their T_{max} were at 670−690 °C, which were much higher than that of CB at approximately 610 °C (Figure S3b, SI). These further confirmed well graphitized struture and relatively high purity for the synthesized CNTs.[39−41]

3.3. Analysis for the Carbonization Mechanism from PP, PE, and PS into CNTs. To further investigate the synergistic effect of CB and Ni$_2$O$_3$, the pyrolysis process of PP, PE and PS was performed (Figure S4, SI).[42] SI Table S2 shows the mass balance relation of pyrolysis products in the PP, PE, and PS system, respectively. Very interestingly, the three systems showed a similar feature. The yield of liquid products increased slightly after incorporation of 5 wt % CB. Upon further addition of 5 wt % Ni$_2$O$_3$, the liquid products decreased greatly and meanwhile, the solid products increased dramatically. This implies that the solid carbon may stem from the carbonization of liquid products. To better comprehend this point, detailed analysis of the composition of the gas and liquid products were conducted by GC and GC-MS (SI Table S3; Figure S5, S6, and S7, SI). The data show that the carbon sources for CNTs can be mainly attributed to the liquid degradation products. In more detail, the liquid products consist mostly of aromatic compounds with lower carbon numbers,

such as benzene, toluene, ethylbenzene, xylene, and naphthalene.

To confirm the relevance of such aromatic liquids with the formation of CNTs, model experiments pertaining to catalyze carbonization of aromatic compounds were designed (Figure 4a). The mass of carbon products from different aromatic compounds is shown in Figure 4b. Under the same conditions, benzene as the carbon resource presented the highest conversion of carbon. More importantly, the yield derived from the combination of CB and Ni_2O_3 is much higher than that from Ni_2O_3 alone. The results revealed that the CB not only played a key role in the degradation of PP, PE, and PS to selectively produce aromatic small molecules, but also took part in the carbonization reaction of the degradation products to form CNTs together with Ni_2O_3.

Based on the above results, a schematic representation for the synergistic mechanism of the combined catalysis in the catalytic conversion of PP, PE, and PS into CNTs is displayed in Figure 5. It highlights two prominent steps. First, these polymers are catalytically degraded by CB during pyrolysis, which changes the composition of liquid products of virgin polymer, producing more aromatic compounds (mainly benzene and its derivatives). In the meantime Ni_2O_3 is reduced to Ni, probably by hydrogen, CB and/or other degradation products. Subsequently, these aromatic molecules are dehydrogenated and catalytically reassembled by CB and Ni to produce more complex aromatic compounds, which in turn serve as the carbon feedstock for the catalytic growth of CNTs from Ni nanoparticles through a vapor−solid−solid growth process as found in CVD grown CNT.[43−48]

3.4. The Application of Synthesized CNTs for Supercapacitors. To evaluate the application of as-synthesized CNTs for supercapacitor, the electrochemical performances were measured. The CV curves of synthesized CNTs at different scan rates are shown in Figure 6a−d. Meanwhile, the C−CNTs and CB were also comparatively investigated (Figure 6e and f). Different from the C−CNTs with a quasirectangular shape, the synthesized CNTs and CB showed some bumps in the CV curves, indicating the contribution of some redox reactions to the electrochemical capacitance.[49]

Figure 7a depicts the specific capacitance (SC) of CNTs and CB. It is apparent that the estimated SC gradually decreased with the increase of scan rate. However, the SC of synthesized CNTs was much higher than that of C−CNT at the same scan rate. For example, the SC values for synthesized CNTs were 100−140 F g^{-1} at 20 mv s^{-1}, but that of C−CNT was only 50 F g^{-1}. Interestingly, the SC from P-E-S was the highest among all synthesized CNTs, implying it is the best candidate for use as an electrode material. Furthermore, the electrochemical stability was also investigated at 10 mV s^{-1} (Figure 7b). All of these electrodes retained high capacitance after 1000 cycles (>98% of initial capacitance). For example, the SC from PP, PE, PS, and P-E-S were 99.5, 98.2, 99.4, and 99.2% of their initial capacitances, respectively. This suggested that the synthesized CNTs had good electrochemical stability as electrode materials for supercapacitors.[50,51]

It is still a puzzle as to why the synthesized CNTs exhibit higher SC than that of C−CNT and CB. The SC of carbon materials is related to its surface area and pore structure,[52,53] so N_2 adsorption−desorption measurements for the above carbon materials were carried out. As summarized in Table 2, the synthesized CNTs had relatively larger BET specific surface areas (S_{BET}) than the C−CNT, but they were smaller than for CB. Moreover, the total pore volume (V_{total}) exhibited a similar
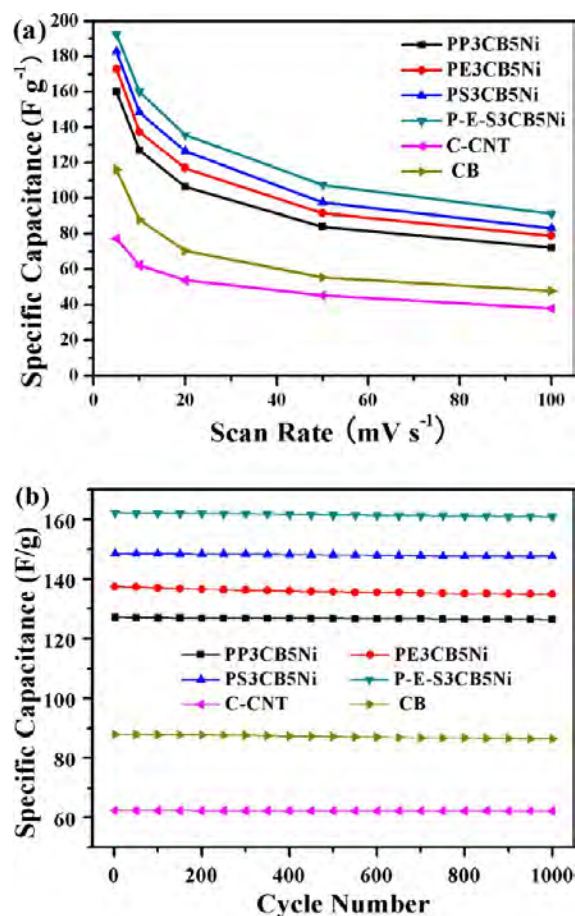
Figure 7. (a) Relationships between the SC values and scan rates for the synthesized CNTs, C−CNTs, and CB; (b) Cycle life of for the synthesized CNTs, C−CNT, and CB at a scan rate of 10 mV s^{-1}.

Table 2. N_2 Adsorption−desorption Isotherm Parameters for the Residual Char of Polymer Samples, Commercial CNT, and CB

sample	S_{BET} $(m^2/g)^a$	V_{total} $(cm^3/g)^b$	DAV $(nm)^c$
PP3CB5Ni	209	1.126	3.836
PE3CB5Ni	366	1.795	3.819
PS3CB5Ni	376	1.342	3.821
P-E-S3CB5Ni	447	1.975	3.822
C−CNT	182	0.590	3.825
CB	943	2.370	3.833

^{a}The total specific surface area. ^{b}The total pore volume. ^{c}The average diameter of pores.

trend to that of S_{BET}, while the average diameter of pores (DAV) of them was very close (approximatly 3.8 nm). These results implied that the specific surface areas and pore structure were not the key factor influencing the SC.

Another important factor to determine the SC of carbon materials was the heteroatom functionalities.[54−56] In the case of oxygen-containing functional groups, pseudocapacitance is generally credited with faradaic reactions of these groups with electrolyte ions.[57,58] XPS was employed to analyze surface elements of the above-mentioned carbon materials. It shows that their surfaces mainly consist of carbon and oxygen without any other elements (Figure S8, SI). Furthermore, XPS C1s core-level spectra were analyzed to determine the chemical

component and oxidation state of carbon element (Figure S9, SI). There were some oxygen-containing groups (C−O, C═O, O═C−O), which might be ascribed to the acid treatment.[59,60] As shown in Table 3, the synthesized CNTs had more oxygen-

Table 3. Percentages of Various Functional Groups from the Residual Char of Polymer Samples, Commercial CNT, and CB

sample	C−C (%)[a]	C−O (%)	C═O (%)	O═C−O (%)
PP3CB5Ni	57.80	20.23	12.14	9.83
PE3CB5Ni	58.82	22.94	8.24	10.00
PS3CB5Ni	55.87	22.35	13.41	8.38
P-E-S3CB5Ni	47.85	30.62	10.53	11.00
C−CNT	66.67	13.33	14.67	5.33
CB	64.94	14.94	10.39	9.74

[a]The percentage of functional groups was calculated according to the integrated area after peak-fit processing.

containing groups than C−CNTs and CB, and the CNTs from P-E-S3CB5Ni had the highest percentage of oxygen-containing groups. The trend was consistent with that of the SC values. Consequently, the improved SC of synthesized CNTs was mainly contributed to the increase of oxygen-containing groups to produce a pseudocapacitance.

In summary, a novel type of "universal" combined catalysts comprising CB and Ni_2O_3, can effectively promote carbonization of polyolefins and PS into CNTs. It is believed that this discovery provides an attractive and useful avenue to dispose of polyolefin wastes to produce high-value CNTs. The combined catalysts are "universal" due to its ability to form CNTs from PP, PE, PS, and their blends. This makes the technique appealing for the large-scale production of CNTs with no need to separate the polyolefin wastes during its recycling. Moreover, the CNTs as electrode material for supercapacitors displayed good electrichemical performance with high specific capacitance.

■ ASSOCIATED CONTENT

Ⓢ Supporting Information
More details on the combustion and pyrolysis equipments, TGA, GC, and GC-MS analysis, and XPS results are available. This material is available free of charge via the Internet at http://pubs.acs.org.

■ AUTHOR INFORMATION

Corresponding Author
*Phone: 86 431 85262004; fax: 86 431 85262827; e-mail: ttang@ciac.ac.cn.

Notes
The authors declare no competing financial interest.

■ ACKNOWLEDGMENTS

■ REFERENCES

(1) Wu, C.; Williams, P. T. Pyrolysis-gasification of plastics, mixed plastics and real-world plastic waste with and without Ni-Mg-Al catalyst. *Fuel* **2010**, *89*, 3022−3032.

(2) Bazargan, A.; McKay, G. A review—Synthesis of carbon nanotubes from plastic wastes. *Chem. Eng. J.* **2012**, *195−196*, 377−391. Bazargan, A.; McKay, G. *Chem. Eng. J.* **2012**, *195−196*, 377−391.

(3) Passamonti, F. J.; Sedran, U. Recycling of waste plastics into fuels. LDPE conversion in FCC. *Appl. Catal., B* **2012**, *125*, 499−506.

(4) Williams, P. T.; Williams, E. A. Fluidised bed pyrolysis of low density polyethylene to produce petrochemical feedstock. *J. Anal. Appl. Pyrol.* **1999**, *51*, 107−126.

(5) Baughman, R. H.; Zakhidov, A. A.; Heer, W. A. D. Carbon nanotubes—The route toward applications. *Science* **2002**, *297*, 787−792.

(6) Paradise, M.; Goswami, T. Carbon nanotubes−Production and industrial applications. *Mater. Des.* **2007**, *28*, 1477−1489.

(7) Popov, V. N. Carbon nanotubes: Properties and application. *Mater. Sci. Eng., R* **2004**, *43*, 61−102.

(8) Oriňáková, R.; Oriňák, A. Recent applications of carbon nanotubes in hydrogen production and storage. *Fuel* **2011**, *90*, 3123−3140.

(9) Zhang, W. D.; Phang, I. Y.; Liu, T. X. Growth of carbon nanotubes on clay: Unique nanostructured filler for high-performance polymer nanocomposites. *Adv. Mater.* **2006**, *18*, 73−77.

(10) Jiang, H.; Lee, P. S.; Li, C. 3D carbon based nanostructures for advanced supercapacitors. *Energy Environ. Sci.* **2013**, *6*, 41−53.

(11) Boukhalfa, S.; Evanoff, K.; Yushin, G. Atomic layer deposition of vanadium oxide on carbon nanotubes for high-power supercapacitor electrodes. *Energy Environ. Sci.* **2012**, *5*, 6872−6879.

(12) Niu, C. M.; Sichel, E. K.; Hoch, R.; Moy, D.; Tennent, H. High power electrochemical capacitors based on carbon nanotube electrodes. *Appl. Phys. Lett.* **1997**, *70*, 1480−1482.

(13) Yoon, B. J.; Jeong, S. H.; Lee, K. H.; Kim, H. S.; Park, C. G.; Han, J. H. Electrical properties of electrical double layer capacitors with integrated carbon nanotube electrodes. *Chem. Phys. Lett.* **2004**, *388*, 170−174.

(14) Dunens, O. M.; MacKenzie, K. J.; Harris, A. T. Synthesis of multiwalled carbon nanotubes on fly ash derived catalysts. *Environ. Sci. Technol.* **2009**, *43*, 7889−7894.

(15) Zhang, Q.; Huang, J. Q.; Zhao, M. Q.; Qian, W. Z.; Wei, F. Carbon nanotube mass production: Principles and processes. *ChemSusChem* **2011**, *4*, 864−889.

(16) Hou, P. X.; Liu, C.; Cheng, H. M. Purification of carbon nanotubes. *Carbon* **2008**, *46*, 2003−2025.

(17) Iijima, S. Helical microtubules of graphitic carbon. *Nature* **1991**, *354*, 56−58.

(18) Guo, T.; Nikolaev, P.; Thess, A.; Colbert, D. T.; Smalley, R. E. Catalytic growth of single-walled manotubes by laser vaporization. *Chem. Phys. Lett.* **1995**, *243*, 49−54.

(19) Thess, A.; Lee, R.; Nikolaev, P.; Dai, H.; Petit, P.; Robert, J.; Xu, C.; Lee, Y. H.; Kim, S. G.; Rinzler, A. G.; Colbert, D. T.; Scuseria, G. E.; Tománek, D.; Fischer, J. E.; Smalley, R. E. Crystalline ropes of metallic carbon nanotubes. *Science* **1996**, *273*, 483−487.

(20) Iijima, S.; Ichlhashi, T. Single-shell carbon nanotubes of 1-nm diameter. *Nature* **1993**, *363*, 603−605.

(21) Cheng, H. M.; Li, F.; Su, G.; Pan, H. Y.; He, L. L.; Sun, X.; Dresselhaus, M. S. Large-scale and low-cost synthesis of single-walled carbon nanotubes by the catalytic pyrolysis of hydrocarbons. *Appl. Phys. Lett.* **1998**, *72*, 3282−3284.

(22) Shen, Y.; Yan, L.; Song, H.; Yang, J.; Yang, G.; Chen, X.; Zhou, J.; Yu, Z. Z.; Yang, S. A general strategy for the synthesis of carbon nanofibers from solid carbon materials. *Angew. Chem., Int. Ed.* **2012**, *51*, 12202−12205.

(23) Hong, N.; Wang, B.; Song, L.; Hu, S.; Tang, G.; Wu, Y.; Hu, Y. Low-cost, facile synthesis of carbon nanosheets by thermal pyrolysis of polystyrene composite. *Mater. Lett.* **2012**, *66*, 60−63.

(24) Chung, Y. H.; Jou, S. Carbon nanotubes from catalytic pyrolysis of polypropylene. *Mater. Chem. Phys.* **2005**, *92*, 256−259.

(25) Zhuo, C. W.; Hall, B.; Richter, H.; Levendis, Y. Synthesis of carbon nanotubes by sequential pyrolysis and combustion of polyethylene. *Carbon* **2010**, *48*, 4024−4034.

4054

dx.doi.org/10.1021/es404646e | *Environ. Sci. Technol.* 2014, 48, 4048−4055

(26) Yang, Z.; Zhang, Q.; Luo, G. H.; Huang, J. Q.; Zhao, M. Q.; Wei, F. Coupled process of plastics pyrolysis and chemical vapor deposition for controllable synthesis of vertically aligned carbon nanotube arrays. *Appl. Phys. A: Mater. Sci. Process.* **2010**, *100*, 533−540.

(27) Tang, T.; Chen, X.; Meng, X.; Chen, H.; Ding, Y. Synthesis of multiwalled carbon nanotubes by catalytic combustion of polypropylene. *Angew. Chem., Int. Ed.* **2005**, *44*, 1517−1520.

(28) Jiang, Z. W.; Song, R. J.; Bi, W. G.; Lu, J.; Tang, T. Polypropylene as a carbon source for the synthesis of multi-walled carbon nanotubes via catalytic combustion. *Carbon* **2007**, *45*, 449−458.

(29) Song, R.; Jiang, Z.; Bi, W.; Cheng, W.; Lu, J.; Huang, B.; Tang, T. The combined catalytic action of solid acids with nickel for the transformation of polypropylene into carbon nanotubes by pyrolysis. *Chem.—Eur. J.* **2007**, *13*, 3234−3240.

(30) Krevelen, D. W. Some basic aspects of flame resistance of polymeric materials. *Polymer* **1975**, *16*, 615−620.

(31) Fitzer, E. Thermal degradation of polymers to polymeric carbon—An approach to the synthesis of new materials. *Angew. Chem., Int. Ed.* **1980**, *19*, 375−385.

(32) Chung, C. K.; Zhou, R. X.; Chang, W. T. The anomalous behavior and properties of Ni−Co films codeposited in the sulfamate-chloride electrolyte. *Microsyst. Technol.* **2008**, *14*, 1279−1284.

(33) Chung, C. K.; Chang, W. T. Effect of pulse frequency and current density on anomalous composition and nanomechanical property of electrodeposited Ni−Co films. *Thin Solid Films* **2009**, *517*, 4800−4804.

(34) Chung, C. K.; Chang, W. T.; Hung, S. T. Electroplating of nickel films at ultra low electrolytic temperature. *Microsyst. Technol.* **2010**, *16*, 1353−1359.

(35) Ma, R. Z.; Xu, C. L.; Wei, B. Q.; Liang, J.; Wu, D. H.; Li, D. J. Electrical conductivity and field emission characteristics of hot-pressed sintered carbon nanotubes. *Mater. Res. Bull.* **1999**, *34*, 741−747.

(36) Jorio, A.; Lucchese, M. M.; Stavale, F.; Ferreira, E. H. M.; Vilani, C.; Moutinho, M. V. O.; Capaz, R. B.; Achete, C. A. Quantifying ion-induced defects and Raman relaxation length in grapheme. *Carbon* **2010**, *48*, 1592−1597.

(37) DiLeo, R. A.; Landi, B. J.; Raffaelle, R. P. Purity assessment of multiwalled carbon nanotubes by Raman spectroscopy. *J. Appl. Phys.* **2007**, *101*, 0643071−0643075.

(38) Wu, C.; Dong, L.; Huang, J.; Williams, P. T. Optimising the sustainability of crude bio-oil via reforming to hydrogen and valuable by-product carbon nanotubes. *RSC Adv.* **2013**, *3*, 19239−19242.

(39) Li, N.; Wang, Z.; Zhao, K.; Shi, Z.; Gu, Z.; Xu, S. Large scale synthesis of N-doped multi-layered graphene sheets by simple arc-discharge method. *Carbon* **2010**, *48*, 255−259.

(40) Xu, D.; Lu, P.; Dai, P.; Wang, H.; Ji, S. In situ synthesis of multiwalled carbon nanotubes over LaNiO$_3$ as support of cobalt nanoclusters catalyst for catalytic applications. *J. Phys. Chem. C* **2012**, *116*, 3405−3413.

(41) Shanov, V.; Cho, W.; Malik, R.; Alvarez, N.; Haase, M.; Ruff, B.; Kienzle, N.; Ochmann, T.; Mast, D.; Schulz, M. CVD growth, characterization and applications of carbon nanostructured materials. *Surf. Coat. Technol.* **2013**, *230*, 77−86.

(42) Wen, X.; Gong, J.; Yu, H.; Liu, Z.; Wan, D.; Liu, J.; Jiang, Z.; Tang, T. Catalyzing carbonization of poly(L-lactide) by nanosized carbon black combined with Ni$_2$O$_3$ for improving flame retardancy. *J. Mater. Chem.* **2012**, *22*, 19974−19980.

(43) Shao, M.; Li, Q.; Wu, J.; Xie, B.; Zhang, S.; Qian, Y. Benzene-thermal route to carbon nanotubes at a moderate temperature. *Carbon* **2000**, *40*, 2961−2973.

(44) Kumar, M.; Ando, Y. Single-wall and multi-wall carbon nanotubes from camphor—A botanical hydrocarbon. *Diamond Relat. Mater.* **2003**, *12*, 1845−1850.

(45) Tian, Y. J.; Hu, Z.; Yang, Y.; Wang, X. Z.; Chen, X.; Xu, H.; Wu, Q.; Ji, W. J.; Chen, Y. In situ TA-MS study of the six-membered-ring-based growth of carbon nanotubes with benzene precursor. *J. Am. Chem. Soc.* **2004**, *126*, 1180−1183.

(46) Deck, C. P.; Vecchio, K. Prediction of carbon nanotube growth success by the analysis of carbon−catalyst binary phase diagrams. *Carbon* **2006**, *44*, 267−275.

(47) Plata, D. L.; Meshot, E. R.; Reddy, C. M.; Hart, A. J.; Gschwend, P. M. Multiple alkynes react with ethylene to enhance carbon nanotube synthesis, suggesting a polymerization-like formation mechanism. *ACS Nano* **2010**, *4*, 7185−7192.

(48) Magrez, A.; Smajda, R.; Seo, J. W.; Horváth, E.; Ribič, P. R.; Andresen, J. C.; Acquaviva, D.; Olariu, A.; Laurenczy, G.; Forró, L. Striking influence of the catalyst support and its acid−base properties: New insight into the growth mechanism of carbon nanotubes. *ACS Nano* **2011**, *5*, 3428−3437.

(49) Zhu, H.; Wang, X.; Yang, F.; Yang, X. Promising carbons for supercapacitors derived from fungi. *Adv. Mater.* **2011**, *23*, 2745−2748.

(50) Simon, P.; Gogotsi, Y. Materials for electrochemical capacitors. *Nat. Mater.* **2008**, *7*, 845−854.

(51) Zhang, L. L.; Zhao, X. S. Carbon-based materials as supercapacitor electrodes. *Chem. Soc. Rev.* **2009**, *38*, 2520−2531.

(52) Niu, C.; Sichel, E. K.; Hoch, R.; Moy, D.; Tennent, H. High power electrochemical capacitors based on carbon nanotube electrodes. *Appl. Phys. Lett.* **1997**, *70*, 1480−1482.

(53) Hiraoka, T.; Izadi-Najafabadi, A.; Yamada, T.; Futaba, D. N.; Yasuda, S.; Tanaike, O.; Hatori, H.; Yumura, M.; Iijima, S.; Hata, K. Compact and light supercapacitor electrodes from a surface-only solid by opened carbon nanotubes with 2200 m^2 g^{-1} surface area. *Adv. Mater.* **2010**, *20*, 422−428.

(54) Zhao, L.; Fan, L. Z.; Zhou, M. Q.; Guan, H.; Qiao, S. Y.; Antonietti, M.; Titirici, M. M. Nitrogen-containing hydrothermal carbons with superior performance in supercapacitors. *Adv. Mater.* **2010**, *22*, 5202−5206.

(55) Frackowiak, E. Carbon materials for supercapacitor application. *Phys. Chem. Chem. Phys.* **2007**, *9*, 1774−1785.

(56) Inagaki, M.; Konno, H.; Tanaike, O. Carbon materials for electrochemical capacitors. *J. Power Sources* **2010**, *195*, 7880−7903.

(57) Conway, B. E.; Birss, V.; Wojtowicz, J. The role and utilization of pseudocapacitance for energy storage by supercapacitors. *J. Power Sources* **1997**, *66*, 1−14.

(58) Qu, D. Studies of the activated carbons used in double-layer Supercapacitors. *J. Power Sources* **2002**, *109*, 403−411.

(59) Nian, Y. R.; Teng, H. Nitric acid modification of activated carbon electrodes for improvement of electrochemical capacitance. *J. Electrochem. Soc.* **2002**, *149*, A1008−A1014.

(60) Oda, H.; Yamashita, A.; Minoura, S.; Okamoto, M.; Morimoto, T. Modification of the oxygen-containing functional group on activated carbon fiber in electrodes of an electric double-layer capacitor. *J. Power Sources* **2006**, *158*, 1510−1516.

Supporting Information

Nanosized carbon black combined with Ni_2O_3 as "universal" catalysts for synergistically catalyzing carbonization of polyolefin wastes to synthesize carbon nanotubes and application for supercapacitors

Xin Wen,[†] Xuecheng Chen,[†,‡] Nana Tian,[†] Jiang Gong,[†] Jie Liu,[†] Mark H. Rümmeli,[§,#] Paul K. Chu,[⊥] Ewa Mijiwska,[‡] and Tao Tang[†,*]

[†]*State Key Laboratory of Polymer Physics and Chemistry, Changchun Institute of Applied Chemistry, Changchun, Jilin 130022, China*

[‡]*Institute of Chemical and Environment Engineering, West Pomeranian University of Technology, Szczecin ul. Pulaskiego 10, 70-322 Szczecin, Poland*

[§]*IBS Center for Integrated Nanostructure Physics, Institute for Basic Science (IBS), Daejon 305-701, Republic of Korea*

[#] *Department of Energy Science, Department of Physics, Sungkyunkwan University, Suwon 440-746, Republic of Korea*

[⊥]Department of Physics and Materials Science, City University of Hong Kong, Tat Chee Avenue, Kowloon, Hong Kong, China

*Corresponding author. E-mail address: ttang@ciac.ac.cn

Table of Contents

This section provides several additional explanations for the main article.

Figure S1. Schematic diagram of the combustion equipment.

Table S1 The carbon yield of polymer composites burned in crucible at 700 ^{o}C.

Figure S2. SEM images for the carbon products from PE/CB/Ni$_2$O$_3$ composites, PS/CB/Ni$_2$O$_3$ and P-E-S/CB/Ni$_2$O$_3$ composites: (a) PE1CB5Ni; (b) PE3CB5Ni; (c) PS1CB5Ni; (d) PS3CB5Ni; (e) P-E-S1CB5Ni; (f) P-E-S3CB5Ni.

Figure S3. (a)TGA and (b)DTG curves of carbon black and synthesized CNTs from polymer composites in air.

Figure S4. Schematic diagram of the catalytic pyrolysis for polymer composites.

Table S2. Yields of pyrolysis products from PP, PE and PS samples at 700 ^{o}C.

Table S3 The compositions of the gas products from PP, PE and PS samples.

**Figure S5.** GC-MS chromatograms of the liquid degradation products from PP and its composites.

Figure S6. GC-MS chromatograms of the liquid degradation products from PE and its composites.

Figure S7. GC-MS chromatograms of the liquid degradation products from PS and its composites.

Figure S8. XPS spectra of the carbon materials from PP3CB5Ni, PE3CB5Ni, PS3CB5Ni, P-E-S3CB5Ni, C-CNT and CB.

Figure S9. XPS C1s core-level spectrum of the CNTs from (a) PP3CB5Ni, (b) PE3CB5Ni, (c) PS3CB5Ni, (d) P-E-S3CB5Ni; (e) C-CNT; and (f) CB.

1. The combustion of polyolefin samples in a crucible.
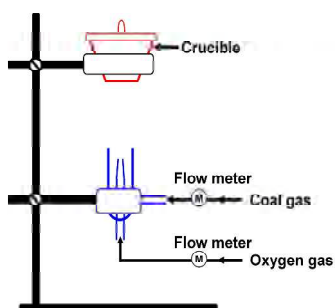
Figure S1. Schematic diagram of the combustion equipment.

**Table S1** The carbon yield of polymer composites burned in crucible at 700 °C.

Sample	Polymer (wt%)			Solid acids (wt%)		Carbon Black (wt%)	Nickel catalyst (wt%)	Yield of carbon[a] (wt%)
	PP	PE	PS	OMC	HZSM			
S1-1 PP/OMC/Ni	100	–	–	5[b]	–	–	5[c]	47.3 ± 1.3
S1-2 PE/OMC/Ni	–	100	–	5[b]	–	–	5[c]	34.1 ± 1.1
S1-3 PS/OMC/Ni	–	–	100	5[b]	–	–	5[c]	4.2 ± 0.1
S1-4 PP-PS/OMC/Ni	90	–	10	5[b]	–	–	5[c]	4.9 ± 0.2
S1-5 PE-PS/OMC/Ni	–	90	10	5[b]	–	–	5[c]	4.8 ± 0.1
S1-6 P-E-S/OMC /Ni	26.9	56.3	16.8	5[b]	–	–	5[c]	4.3 ± 0.1
S2-1 PP/HZSM/Ni	100	–	–	–	5[d]	–	5[e]	45.2 ± 0.9
S2-2 PE/HZSM/Ni	–	100	–	–	5[d]	–	5[e]	37.2 ± 0.9
S2-3 PS/HZSM/Ni	–	–	100	–	5[d]	–	5[e]	2.8 ± 0.1
S2-4 PP-PS/HZSM/Ni	90	–	10	–	5[d]	–	5[e]	5.7 ± 0.2
S2-5 PE-PS/HZSM/Ni	–	90	10	–	5[d]	–	5[e]	5.3 ± 0.1
S2-6 P-E-S/HZSM/Ni	26.9	56.3	16.8	–	5[d]	–	5[e]	5.2 ± 0.1

[a]Yield of carbon: the amounts of residual catalysts were subtracted; [b]OMC: organic-modified clay (Nanomer, trademark 1.30P); [c]Ni catalyst (Ni-cat; supported on silica–alumina, Ni content ≈ 66%, Alfa Aesar);[d]HZSM-5: H-form ZSM-5 molecular sieves (Si/Al = 38, d <10 um); [e]Ni_2O_3.

The combustion equipment used is illustrated in Figure S1. To obtain a steady combustion temperature in the crucible, the distance from the top of gas lamp to the bottom of crucible was fixed (140 mm), and the flow rates for coal gas and oxygen were kept at 0.40 and 1.20 ml/min, respectively. The combustion temperature was measured by Pt–Rh thermocouple. The samples were rapidly put into the crucible at a determined temperature and the crucible lid quickly placed. The crucible was taken from the flame when the yellow flame disappeared (about 5–7 min) and was cooled to room temperature. Afterward, the lid was taken away, and then the charred residue was weighed.

## 2. Morphologies of carbon products from PE and polyolefin blends.
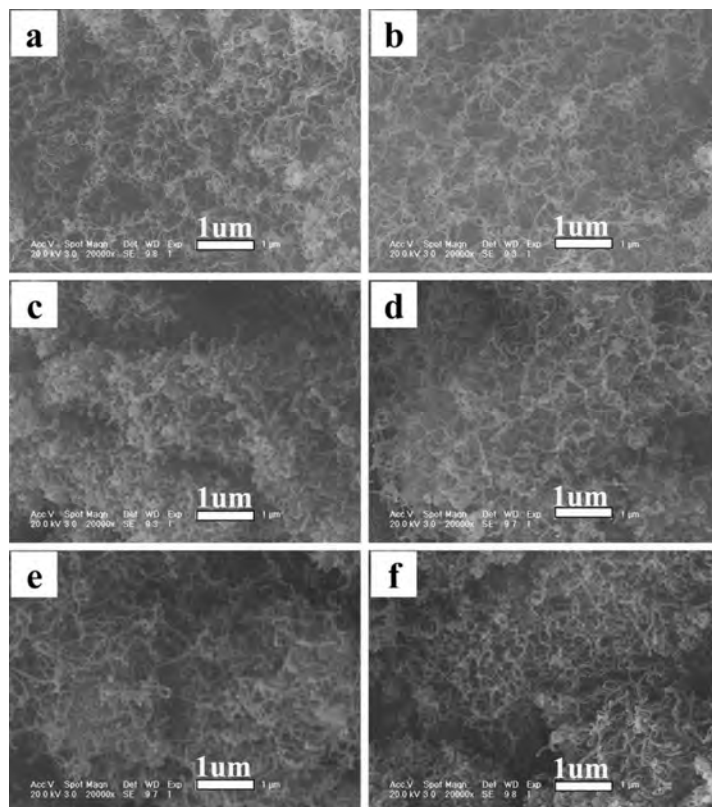
Figure S2. SEM images for the carbon products from PE/CB/Ni$_2$O$_3$ composites, PS/CB/Ni$_2$O$_3$ and P-E-S/CB/Ni$_2$O$_3$ composites: (a) PE1CB5Ni; (b) PE3CB5Ni; (c) PS1CB5Ni; (d) PS3CB5Ni; (e) P-E-S1CB5Ni; (f) P-E-S3CB5Ni.

3. TGA for carbon black and the synthesized CNTs.
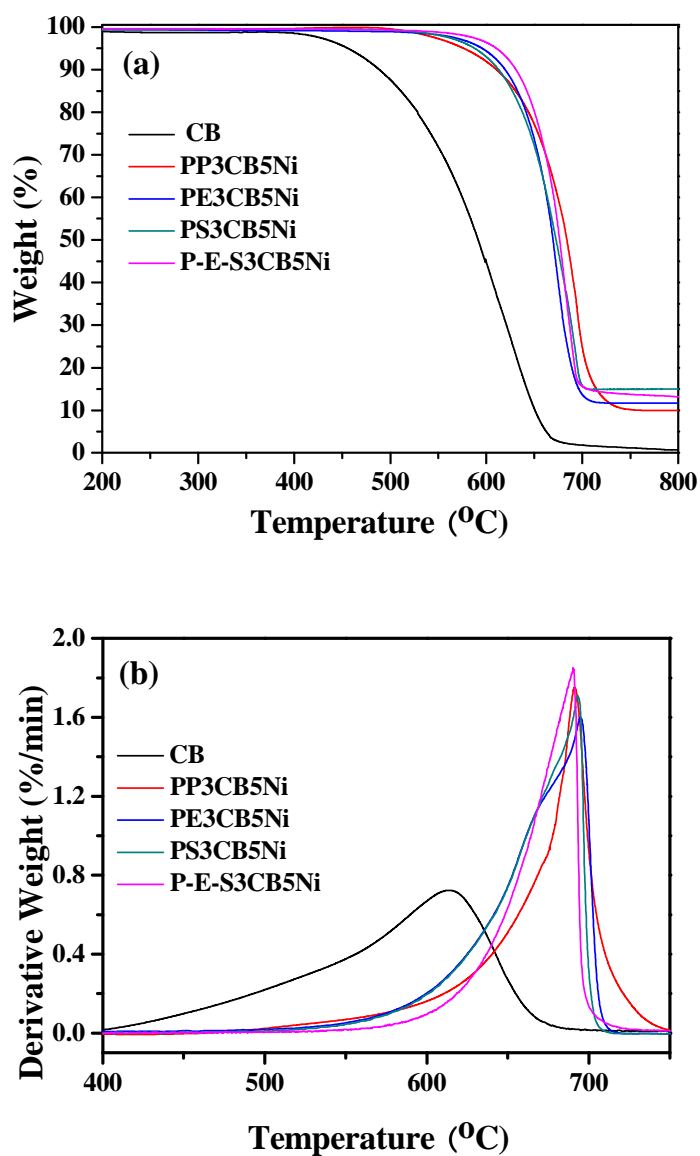
Figure S3. (a)TGA and (b)DTG curves of carbon black and synthesized CNTs from polymer composites in air.

4. The catalytic pyrolysis of polyolefin samples in a quartz tube.
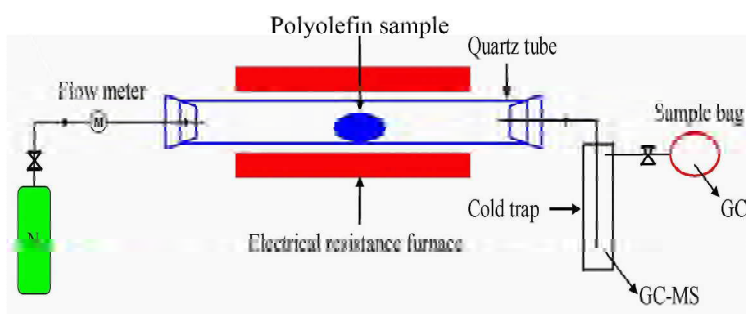
Figure S4. Schematic diagram of the catalytic pyrolysis for polymer composites.

The catalytic pyrolysis setup used is provided in Figure S4. The pyrolysis temperature was controlled by an electrical resistance furnace. The sample was placed in the quartz tube with an internal diameter of 30 mm. Initially the system was flushed with nitrogen with a flow of 200 ml/min for 10 minutes. When the temperature reached to 700 °C, the quartz tube was rapidly put into the furnace. The gas products were collected in the sample bag, and the liquid products were stored in the cold trap.

Table S2. Yields of pyrolysis products from PP, PE and PS samples at 700 °C.

Sample	Yield[a] (/g PS)		
	Solid (wt%)[b]	Liquid (wt%)	Gas(wt%)[c]
PP	0	51.9	48.1
PP5CB	1.6	58.5	39.9
PP5CB5Ni	28.9	23.7	47.4
PE	0	38.2	61.8
PE5CB	1.3	43.3	55.4
PE5CB5Ni	21.5	19.9	58.6
PS	0	62.4	37.6
PS5CB	0.9	66.2	32.9
PS5CB5Ni	18.3	46.9	34.8

[a]Normalization processing were applied to calculate the yield; [b]The mass of the residual catalysts were subtracted; [c]Calculate according to the mass balance.

**4.1 GC analysis for the gas products**

To identify whether the carbon sources were mainly from small molecular gases, GC was employed to analyze in detail the compositions of the gas degradation products for the PP, PE and PS systems, respectively. As shown in Table S3, the gas degradation products from them mainly consisted of hydrogen, methane, ethane, ethylene, propane, and propylene. Although the content of each gas was different due to the different chemical structure of polyolefin, a similar trend was present for the change of the total alkane and olefin in the three systems. When 5 wt% CB was added, the total vol% of alkane gases slightly increased, meanwhile the total vol% of olefin gases decreased somewhat. The total vol% of both alkane and olefin gases decreased remarkably in the systems consisting of CB and Ni_2O_3, which was attributed to the increase of hydrogen content. Researchers report that small molecular gases (such as methane, ethane, ethylene, propane, and propylene, etc.) can be used as carbon sources to synthesize CNTs by CVD. The ratio of alkane and olefin gases changed only a little in our systems. This suggested that gas degradation products were not the main carbon sources for the growth of CNTs. Combining with the above results (Table S2), it is believed that the carbon sources were mainly from liquid degradation products. Therefore, the composition of liquid products was analyzed by GC-MS chromatograms, which will be discussed in the next section.

Table S3 The compositions of the gas products from PP, PE and PS samples.

| Gas products	Vol (vol%)[a]								
	PP	PP5CB	PP5CB5Ni	PE	PE5CB	PE5CB5Ni	PS	PS5CB	PS5CB5Ni
H_2	11.36	13.72	40.39	9.08	11.12	33.47	19.49	13.93	36.29
CH_4	32.56	36.05	31.58	26.99	28.71	24.92	47.77	53.90	37.08
C_2H_6	8.29	7.88	4.26	6.40	6.24	5.31	1.64	2.19	0.78
C_2H_4	21.02	19.34	14.16	39.03	37.05	21.37	27.46	26.85	22.56
C_3H_8	1.23	1.18	0.63	1.33	1.09	0.96	0.09	0.18	0.08
C_3H_6	24.25	19.44	7.16	13.18	12.56	10.61	2.08	2.33	0.57
i-C_4H_{10}	0.09	0.07	0.03	0.19	0.15	0.14	0.04	0.09	0.14
n-C_4H_{10}	0.02	0.04	0.05	1.74	1.27	1.11	0.04	0.18	0.07
n-C_4H_8	0.18	0.19	0.10	0.17	0.17	0.14	0.04	0.09	0.14
i-C_4H_8	0.32	1.66	0.92	0.10	0.13	0.10	0.09	0.09	0.07
cis-C_4H_8	0.18	0.13	0.10	1.20	1.18	1.01	0.04	0.18	0.07
i-C_5H_{12}	0.14	0.06	0.02	0.07	0.04	0.03	0.04	0.09	0.07
n-C_5H_{12}	0.11	0.11	0.02	0.42	0.01	0.02	0.09	0.09	0.14
C_5H_{10}	0.02	0.06	0.00	0.02	0.17	0.14	0.04	0.09	0.07
CO	0.23	0.09	0.58	0.08	0.11	0.67	1.02	0.95	1.87
Total of Alkane	42.44	45.38	36.58	37.14	37.52	32.50	49.72	56.71	37.36
Total of Olefin	45.97	40.81	22.45	53.70	51.25	33.37	29.77	29.61	23.48
Total gases	100.00	100.00	100.00	100.00	100.00	100.00	100.00	100.00	100.00

[a] Calculated by the volume of the gas divided by the total of gas products.

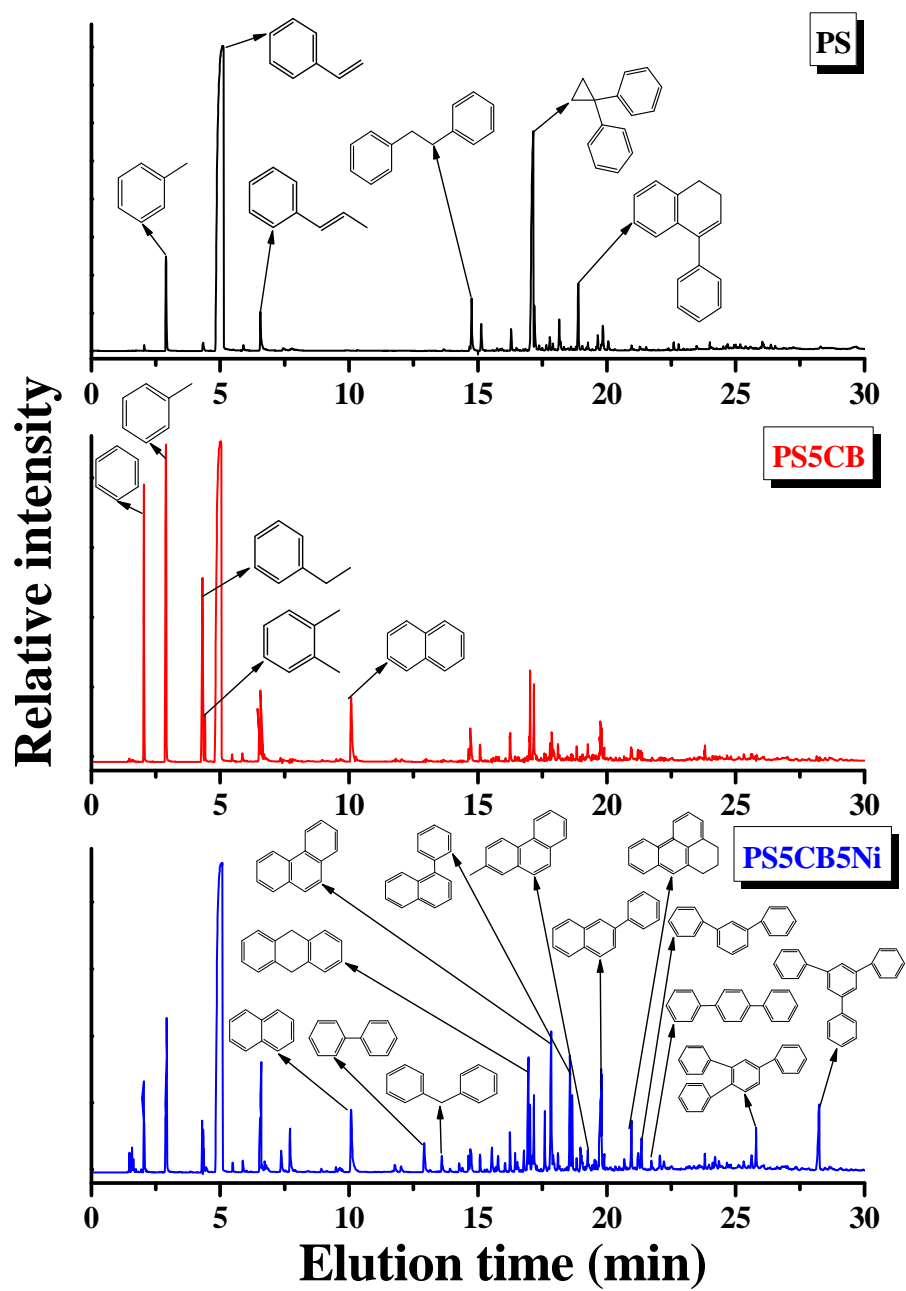**4. 2 GC-MS analysis for the liquid products**
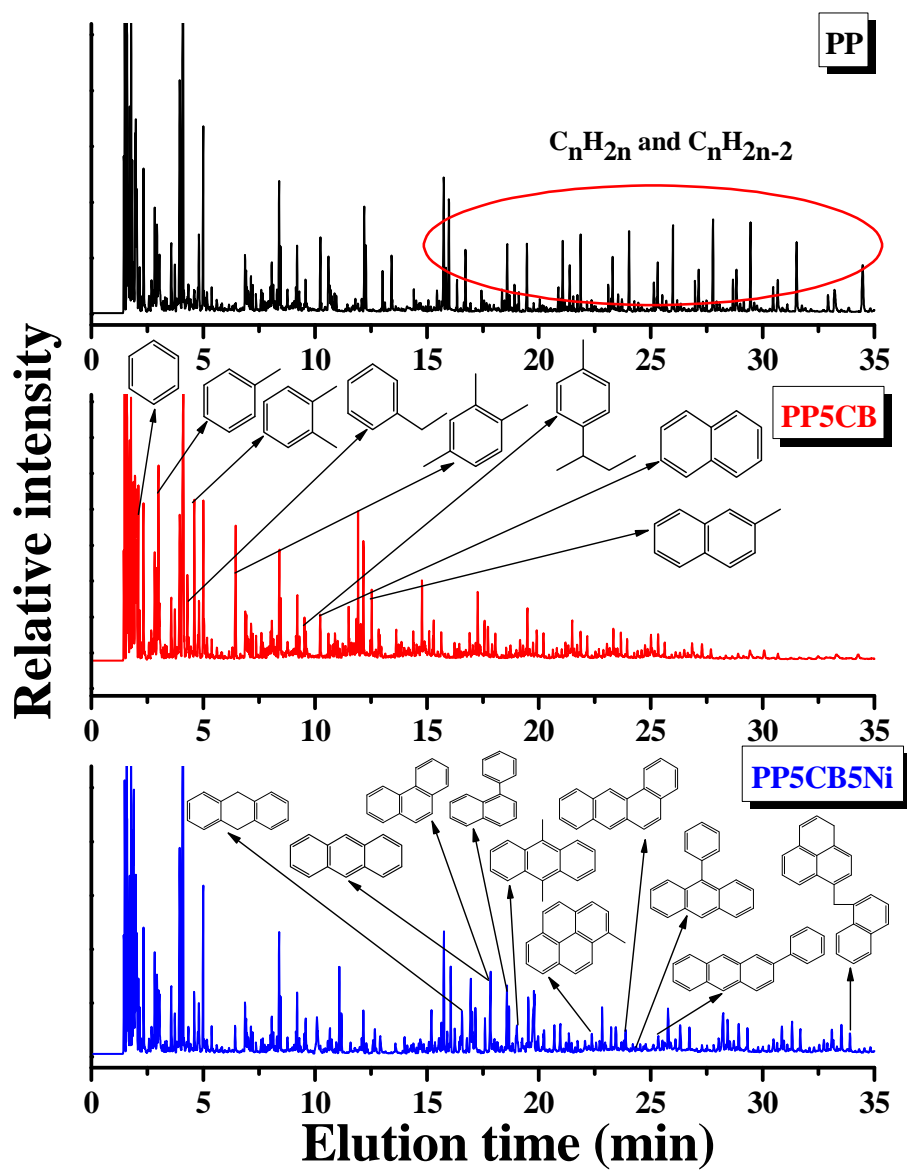
Figure S5. GC-MS chromatograms of the liquid pyrolysis products from PP and its composites.
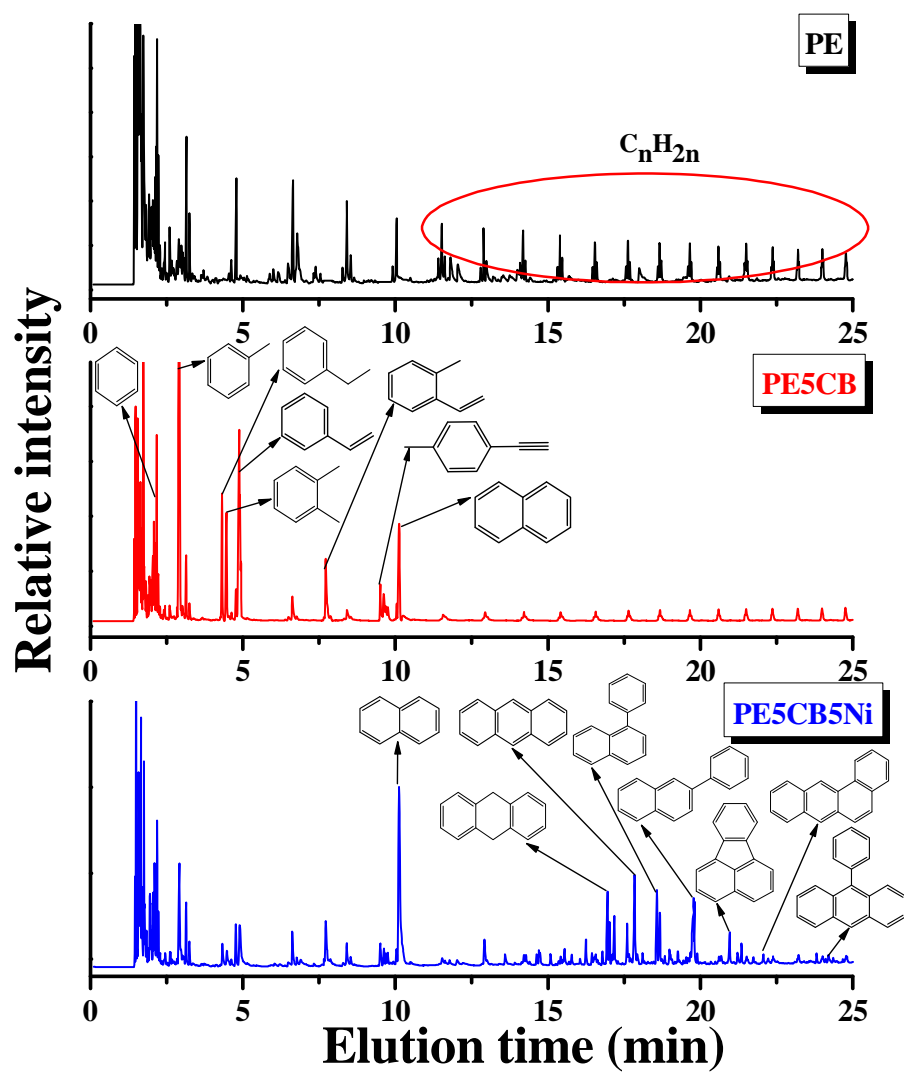
Figure S6. GC-MS chromatograms of the liquid pyrolysis products from PE and its composites.

Figure S7. GC-MS chromatograms of the liquid pyrolysis products from PS and its composites.

Figure S5 shows the composition of the liquid products from PP systems by GC-MS. Pristine PP contains not only many light hydrocarbons, but also lots of long-chain olefins (C_nH_{2n}) and diolefins (C_nH_{2n-2}). After adding 5wt% CB into PP, the content of long-chain olefins and diolefins decreased greatly and aromatic compounds with low carbon numbers (such as benzene, toluene, xylene and ethylbenzene) became the main components. In the PP5CB5Ni system, the relative intensity of these aromatic compounds became weaker, but some new aromatic compounds with higher carbon numbers were produced, implying that the aromatic compounds with low carbon numbers may be the carbon sources.
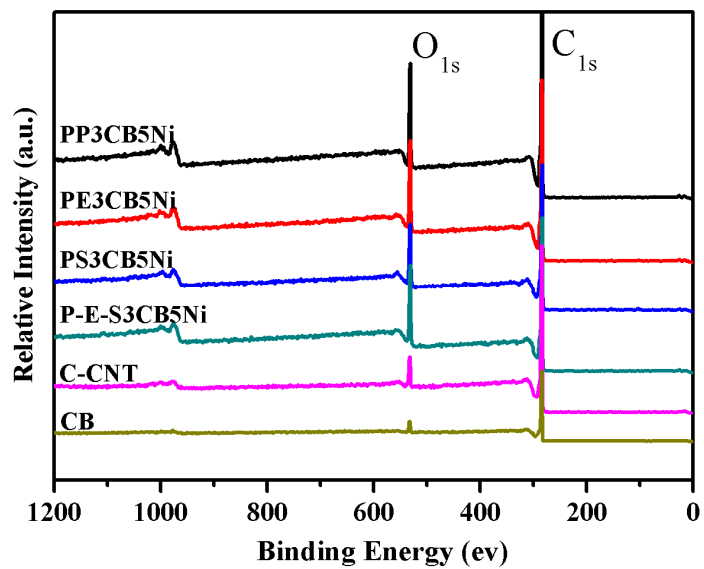
A similar phenomenon was observed in the PE systems (Figure S6). The intensity of long-chain olefins (C_nH_{2n}) decreased greatly in PE5CB and it produced some aromatic compounds with low carbon numbers. The content of these aromatic compounds decreased in PE5CB5Ni and consisted of some new aromatic compounds with higher carbon numbers.

A similar tend was also found from the PS systems (Figure S7). Although the pyrolysis products contained some aromatic compounds with lower carbon numbers (such as benzene, toluene and xylene) for neat PS, their contents were significantly increased in PS5CB. Then the content of these aromatic compounds decreased in PS5CB5Ni, while that of some new aromatic compounds with higher carbon numbers increased.
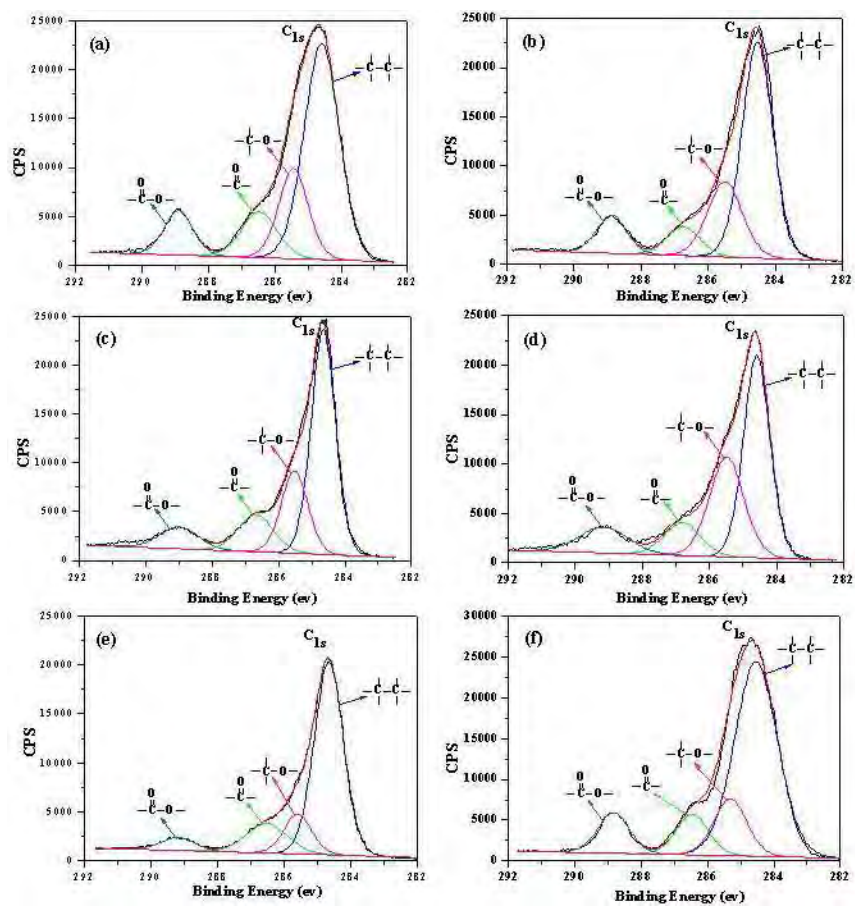
4. 3 Morphology and structure of residual chars

The morphology and structure of the residual chars were examined by SEM, TEM, and XRD. The results indicated that the chars were amorphous carbon from the samples only consisting of CB, but the chars from CB/Ni_2O_3 composites were multi-walled carbon nanotubes. These results were well consistent with the morphology and structure of residual chars from the crucible.

5. XPS spectra of the synthesized CNT, C-CNT and CB.

Figure S8. XPS spectra of the carbon materials from PP3CB5Ni, PE3CB5Ni, PS3CB5Ni, P-E-S3CB5Ni, C-CNT and CB.

Figure S9. XPS C1s core-level spectrum of the CNTs from (a) PP3CB5Ni, (b) PE3CB5Ni, (c) PS3CB5Ni, (d) P-E-S3CB5Ni; (e) C-CNT; and (f) CB.